第 92 卷 第 11 期
2018年11月 2215～2226

地 质 学 报 ACTA GEOLOGICA SINICA

Vol. 92 No. 11 2018
Nov. 2215～2226

冈底斯带西北缘别若则错地区晚白垩世闪长岩 LA-ICP-MS 锆石 U-Pb 测年、地球化学及地质意义

邱婵媛[1)]，肖倩茹[1)]，魏永峰[1,2)]，罗巍[1,2)]，杨亚民[1)]，肖渊甫[1)]

1）成都理工大学地球科学学院，成都，610059；

2）四川省地质矿产勘查开发局区域地质调查队，四川双流，610213

内容提要：别若则错地区闪长岩体呈不规则状、近椭圆状岩株侵位于早白垩世去申拉组或中酸性岩体中，内部可见少量暗色镁铁质包体。通过对闪长岩进行 LA-ICP-MS 锆石 U-Pb 测年，获得 81.4±0.9Ma（MSWD＝0.55）岩石结晶年龄，确认形成时代为晚白垩世。岩石具高 K_2O、低 CaO 特征，为准铝质高钾钙碱性系列岩石（KCG）。稀土元素总量为 113.80×10^{-6}～197.28×10^{-6}，$(La/Yb)_N$ 为 11.98～20.26，δEu＝0.83～0.98，球粒陨石标准化稀土元素配分模式表现为 LREE 相对富集的右倾分布，Eu 亏损不明显；在原始地幔标准化比值蛛网图上，富集 K、Rb，亏损 Ba、Nb、P、Ce，类似于弧型火山岩。闪长岩地球化学成分具有明显的地幔和新生地壳双重特征，说明区内该类岩石是在地幔软流底辟作用下，由前期俯冲和碰撞间产生的地壳发生线性热隆及薄化减压、地幔热能和物质参与了地壳部分熔融和热隆伸展形成，形成环境为班公湖-怒江洋陆转换后碰撞伸展环境。

关键词：冈底斯带西北缘；晚白垩世；闪长岩；LA-ICP-MS 锆石 U-Pb 测年

冈底斯构造岩浆带是发育于青藏高原中南部，印度河-雅鲁藏布缝合带（IYZSZ）与班公湖-怒江缝合带（BNSZ）之间的一条近东西向展布的巨型构造-岩浆带，带内广泛分布着中生代岩浆岩（Mo Xuanxue et al.，2005；Zhu Dicheng et al.，2008b）（图 1a）。对冈底斯带内中生代岩浆岩成因、构造环境已取得较丰富成果（Pearce et al.，1988；Harris et al.，1990；Pan Guitang et al.，2006；Zhu Dicheng et al.，2006，2008a，2008b，Zhe et al.，2009，2011；Kapp et al.，2007；Kang Zhiqiang et al.，2008；Kang Zhiqiang et al.，2009；Liu Wei et al.，2010；Shui Xinfang et al.，2016；Zeng Zhongcheng et al. 2016；Zhou Hua et al.，2016；Yi Mingxiao et al.，2017；Liu Yufei et al.，2018）。受系统的、高质量的年代学和地球化学数据约束（Zhang Yujie et al.，2014），冈底斯地质构造属性迄今存在着不同的认识，有学者认为侏罗纪受班公湖-怒江洋壳的向南消减而处于沟弧盆演化阶段，早白垩世进入碰撞或后碰撞阶段（Pearce et al.，1988；Coulon et al.，1986；Harris et al.，1990）；另有学者认为该区在整个侏罗纪—早白垩世处于弧盆系演化阶段，晚白垩世表现为冈底斯地块与羌塘地块之间的碰撞（Pan Guitang et al.，2006；Kang Zhiqiang et al.，2008，2009；Liu Wei et al.，2010）；此种情况制约着冈底斯乃至青藏高原南部地质构造演化的研究（Li Fenqi et al.，2004）。辉长质-闪长质-花岗闪长质岩石记录了岩石圈与地壳相互作用的丰富信息，已为探索花岗岩类岩石岩浆起源与深部作用过程的重要研究对象（Turner，1996；Meng Fancong et al.，2005）。本文通过对西藏改则别若则错地区晚白垩世闪长岩的 LA-ICS-MS 锆石 U-Pb 精确定年，结合地球化学特征分析，讨论了闪长岩成因和区域构造演化过程，为全面认识冈底斯中北部晚白垩世岩浆活动及深入研究冈底斯中生代区域构造演化提供了新的证据，对探讨冈底斯中生代构造-岩浆作用具有一定的意义。

1 地质概况及岩石学特征

别若则错地区晚白垩世闪长岩体位于北冈底斯与中冈底斯过渡部位（图 1），北冈底斯带内以发育

注：本文为西藏改则别若则错 1∶5 万（I44E022020、I44E022021、I44E023020、I44E023021）4 幅地质矿产调查项目（编号 12120113036600）资助成果。

收稿日期：2018-04-28；改回日期：2018-08-14；责任编辑：周健。

作者简介：邱婵媛，女，1990 年生。硕士研究生，矿物学、岩石学、矿床学专业。Email：m17748490715@163.com。通讯作者：肖倩茹，女，1987 年生。博士研究生，矿物学、岩石学、矿床学专业。Email：18628183715@163.com。

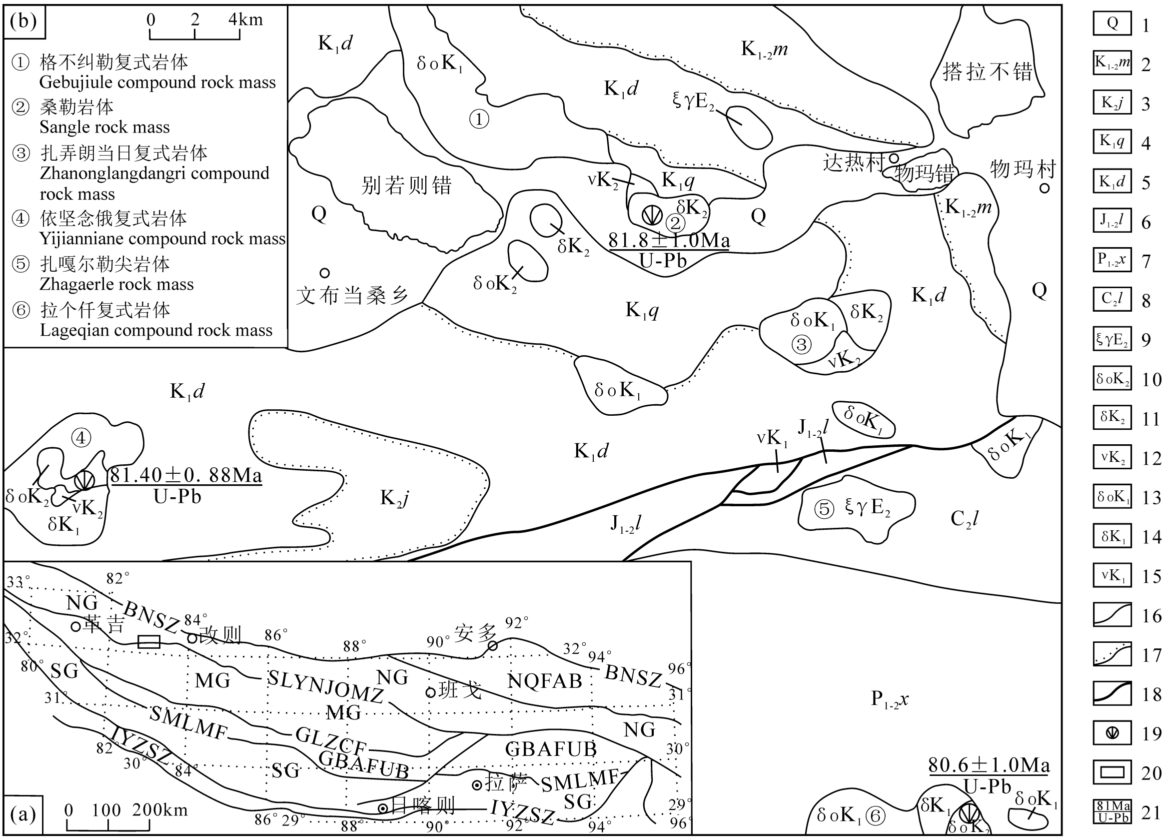

图 1 冈底斯构造单元划分(a)(据朱弟成等,2008)及别若则错地区地质简图(b)

Fig. 1 Geological sketch map showing tectonic unit division of Gangdise (a) (after Zhu Dicheng et al., 2008) and simplified geological map of the Bieruozecuo area (b)

1—第四系;2—早—晚白垩世美苏组;3—晚白垩世竟柱山组;4—早白垩世去申拉组;5—早白垩世多尼组;6—早—中侏罗世拉贡塘组;7—早—晚二叠世下拉组;8—晚石炭世拉嘎组;9—中始新世钾长花岗岩;10—晚白垩世石英闪长岩;11—晚白垩世闪长岩;12—晚白垩世辉长岩;13—早白垩世石英闪长岩;14—早白垩世闪长岩;15—早白垩世辉长岩;16—地质界线;17—角度不整合界线;18—断层;19—测年样品采集位置;20—研究区位置;21—同位素年龄/测试方法;NQFAB—那曲弧前盆地;NG—北冈底斯;MG—中冈底斯;GBAFUB—冈底斯弧背断隆带;SG—南冈底斯;SMLMF—沙莫勒-麦拉-洛巴堆-米拉山断裂;GLZCF—噶尔-隆格尔-扎日南木错-措麦断裂带;SLYNJOMZ—狮泉河-拉果错-永珠-纳木错-嘉黎蛇绿混杂岩带;BNSZ—班公湖-怒江缝合带;IYZSZ—印度河-雅鲁藏布缝合带

1—Quaternary; 2—Early-Late Cretaceous Meisu Formation; 3—Late Cretaceous Jingzhushan Formation; 4—Early Cretaceous Qushenla Formation; 5—Early Cretaceous Doni Formation; 6—Early-Middle Jurassic Lagongtang Formation; 7—Early-Late Permian Xiala Formation; 8—Late Carboniferous Epoch Laga Formation; 9—Middle Eocene moyite; 10—Late Cretaceous quartz diorite; 11—Late Cretaceous diorite; 12—Late Cretaceous gabbro; 13—Early Cretaceous quartz diorite; 14—Early Cretaceous diorite; 15—Early Cretaceous gabbro; 16—geological boundary; 17—angle unconformity boundary; 18—fault; 19—dating sampling spot; 20—studied area; 21—isotopic age/test method; NQFAB—Naqu fore-arc basin; NG—North Gangdise; MG—Middle Gangdise; GBAFUB—Gangdise back-arc fault-uplift belt; SG—South Gangdise; SMLMF—Shamole-Maila-Luobadui-Milashan fault; GLZCF—Ge'e-Longge'e-Zharinanmucuo-Cuomai fault; SLYNJOMZ—Shiquanhe-Laguocuo-Yongzhu-Namucuo-Jiali ophiolitic melange zone; BNSZ—Bangonghu-Nujiang suture zone; IYZSZ—Indus-Yarlung Zangbo suture zone

侏罗系—白垩系火山沉积地层及大量基—中酸性侵入岩为特征;中冈底斯带内发育早—晚二叠世下拉组碳酸盐岩及晚石炭世拉嘎组碎屑岩。晚白垩世闪长岩体呈不规则状、近椭圆状等岩株侵位于早白垩世去申拉组或早白垩世中酸性岩体中,单个岩体出露面积 15.0～21.3km^2,岩体的外接触带有较明显的角岩化、硅化、大理岩化、绿泥石化等热接触变质现象。岩体内可见少量暗色镁铁质包体,其与寄主岩之间接触清晰,呈浑圆状,大小为 15～110mm,无明显定向。岩体岩性主要为闪长岩、石英闪长岩,少量辉长岩、花岗闪长岩、二长花岗岩及正长花岗岩,(石英)闪长岩呈灰白—灰绿色,细—中粒半自形粒状结构,主要由斜长石及角闪石组成,其中斜长石(～80%)为中长石及拉长石,呈半自形板状,粒径一般为 0.2～1.3mm;钾长石(～5%)为正长石,呈半自形板状;角闪石(～12%)为普通角闪石,半自形柱

状；石英（～15％）为他形粒状，含少量锆石、磷灰石、磁铁矿等副矿物。

2　样品处理及分析测试

岩石主量、稀土及微量元素测试样品加工由华阳地矿检测中心实验室完成，测试由国土资源部武汉矿产资源监督检测中心武汉综合岩矿测试中心完成，主量元素、微量元素、稀土元素采用 AXIOS X 射线荧光光谱仪、X Series2 等离子质谱仪、IRIS Intripid2XSP ICP 全谱直读光谱仪、ZEEnit600 石墨炉原子吸收光谱仪、AFS-230E 原子荧光分光光度计分析。测年样品的清洗、粉碎、分选由四川华阳岩矿测试中心完成，西北大学大陆动力学国家重点实验室进行阴极发光（CL）图像采集及 LA-ICP-MS 锆石 U-Pb 测年。测年采用国际标准锆石 91500 外部校正法进行校正。激光器为 ArF193nm 紫外准分子激光器，单脉冲能量 220mJ，最高重复频率 20Hz，经光学系统匀光和聚焦，能量密度可达 20J/cm^2，剥蚀直径 20μm 左右。为了控制仪器的稳定性及控制测试精度，每测试分析 5 个测点后测定标准样 1 次。数据处理采用 ISOPLOT（ver2.49）和 GLITTER（ver4.0，Macquarie University）软件程序。详细分析流程和原理参见 Hou Kejun et al.（2009）。

3　锆石 U-Pb 年代学

测年样品 P12(74) 取自依坚念俄复式岩体，选取 24 粒锆石进行了 LA-ICP-MS 法 U-Pb 测年，分析锆石为无色—浅黄色，颗粒形状规则，主要表现为柱状自形晶，粒径多为 90～140μm，个别可达 180μm，长宽比为 1.8∶1～3.2∶1。锆石 CL 图像表现出典型的岩浆韵律环带和明暗相间的条带结构，属无核岩浆结晶锆石，可代表闪长岩成岩年龄。获得测试数据见表 1，样品的谐和曲线均剔除了严重偏离谐和线数据。样品 24 粒锆石 18 个分析点集中分布于谐和线上或附近（图 2a），$^{206}Pb/^{238}U$ 加权平均年龄为 81.4±0.9Ma（MSWD＝0.55），可代表样品形成年龄，形成时代为晚白垩世。另两个闪长岩样品（图 1b）的 $^{206}Pb/^{238}U$ 加权平均年龄分别为 81.8±1.0Ma（MSWD＝0.94）和 80.6±1.0Ma（MSWD＝0.94）❶，年龄误差范围一致。

4　岩石地球化学

4.1　主量元素

研究区该期闪长岩主量元素分析结果见表 2。由分析结果可见，SiO_2 含量为 55.02％～62.77％、Al_2O_3 为 15.84％～17.04％、K_2O 为 2.28％～3.21％、Na_2O 为 3.57％～5.28％、MgO 为 2.39％～3.80％、TiO_2 为 0.591％～1.280％、P_2O_5 为 0.227％～0.414％。全碱 ALK＝6.34％～7.60％，Na_2O/K_2O＝1.11～2.28，略富钠，岩石铝饱和度 A/CNK＝0.71～0.88，里特曼指数 σ 为 2.72～4.50，CIPW 计算结果表明，仅有 P04(29) 样品中含有标准矿物刚玉分子（0.38），其他样品中不含。在 SiO_2-K_2O 图解中（图 3a），样品主要落在高钾钙碱性区域，在 A/NK-A/CNK 图上（图 3b），样品均落入准铝质岩区域。石英闪长岩与闪长岩相比有更高的 SiO_2、Na_2O 及略低的 K_2O、MgO、TiO_2、P_2O_5 含量。主量元素显示该地区晚白垩世闪长岩类岩石为准铝质高钾钙碱性系列岩石。

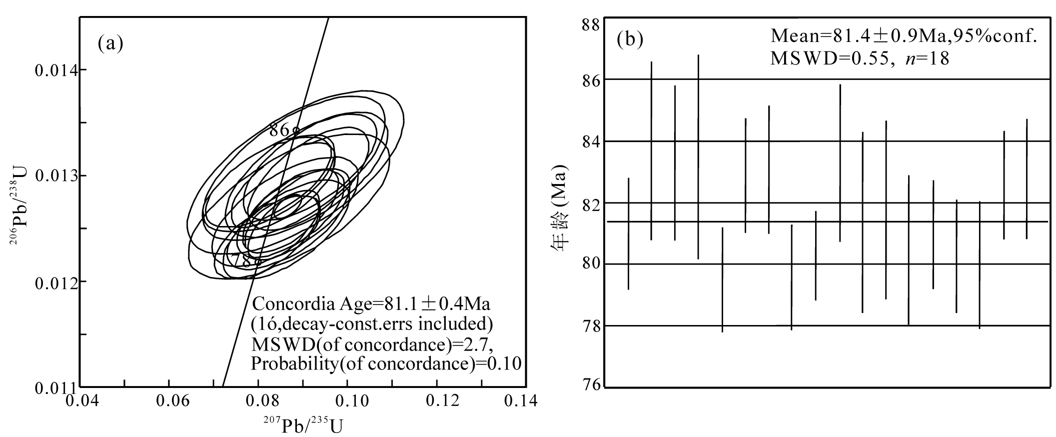

图 2　别若则错地区晚白垩世闪长岩 LA-ICP-MS 锆石 U-Pb 测年谐和图及直方图

Fig. 2　Concordia diagram and histogram showing LA-ICP-MS zircon U-Pb dating for the Late Cretaceous diorite from Bieruozecuo area

表 1 别若则错地区晚白垩世闪长岩 LA-ICP-MS 锆石 U-Pb 同位素分析数据

Table 1 Parameters of LA-ICP-MS zircon U-Pb isotopic analyses for the Late Cretaceous diorite from Bieruozecuo area

点号	同位素比值								年龄(Ma)							
	$^{207}Pb/^{206}Pb$		$^{207}Pb/^{235}U$		$^{206}Pb/^{238}U$		$^{208}Pb/^{232}Th$		$^{207}Pb/^{206}Pb$		$^{207}Pb/^{235}U$		$^{206}Pb/^{238}U$		$^{208}Pb/^{232}Th$	
	比值	1σ	比值	1σ	比值	1σ	比值	1σ	年龄	1σ	年龄	1σ	年龄	1σ	年龄	1σ
P12(74)-01	0.05084	0.00474	0.08865	0.00774	0.01264	0.00028	0.00392	0.00013	233.5	201.9	86.2	7.2	81.0	1.8	79.0	2.5
P12(74)-02	0.09982	0.00744	0.18676	0.01247	0.01356	0.00031	0.00601	0.00021	1620.8	132.7	173.9	10.7	86.9	1.9	121.1	4.1
P12(74)-03	0.04821	0.01313	0.09255	0.02464	0.01392	0.00076	0.00541	0.00056	109.7	541.5	89.9	22.9	89.1	4.8	109.1	11.3
P12(74)-04	0.04873	0.00776	0.08783	0.01352	0.01307	0.00045	0.00443	0.00026	134.8	336.1	85.5	12.6	83.7	2.8	89.4	5.3
P12(74)-05	0.05069	0.00575	0.09141	0.00987	0.01308	0.00033	0.00411	0.00017	226.6	242.1	88.8	9.2	83.7	2.1	82.9	3.5
P12(74)-06	0.04908	0.00916	0.08822	0.01598	0.01303	0.00051	0.00460	0.00034	151.9	386.4	85.8	14.9	83.5	3.3	92.7	6.8
P12(74)-07	0.04713	0.02253	0.09390	0.04404	0.01445	0.00137	0.00572	0.00094	55.3	863.0	91.1	40.9	92.5	8.7	115.3	18.9
P12(74)-08	0.04842	0.00448	0.08291	0.00719	0.01242	0.00026	0.00376	0.00012	120.1	204.6	80.9	6.7	79.5	1.7	75.9	2.4
P12(74)-09	0.04602	0.00543	0.08212	0.00932	0.01294	0.00028	0.00424	0.00016	0.1	261.2	80.1	8.7	82.9	1.8	85.5	3.3
P12(74)-10	0.05100	0.00530	0.09120	0.00894	0.01297	0.00032	0.00410	0.00016	240.7	222.6	88.6	8.3	83.1	2.0	82.6	3.2
P12(74)-11	0.04775	0.00476	0.08178	0.00772	0.01242	0.00026	0.00407	0.00015	85.9	221.8	79.8	7.3	79.6	1.7	82.1	2.9
P12(74)-12	0.05018	0.00369	0.09345	0.00626	0.0135	0.00025	0.00441	0.00011	203.3	162.3	90.7	5.8	86.5	1.6	89	2.2
P12(74)-13	0.04957	0.00340	0.08564	0.00528	0.01253	0.00022	0.00396	0.00009	175.1	152.6	83.4	4.94	80.3	1.4	79.9	1.9
P12(74)-14	0.05047	0.00695	0.09057	0.01200	0.01301	0.00039	0.00434	0.00022	216.7	290.8	88	11.2	83.3	2.5	87.6	4.4
P12(74)-15	0.04951	0.00873	0.08678	0.01486	0.01271	0.00045	0.00437	0.00027	172.1	366.1	84.5	13.9	81.4	2.9	88.1	5.5
P12(74)-16	0.04920	0.00645	0.08591	0.01083	0.01266	0.00034	0.00414	0.00019	157.6	280.7	83.7	10.1	81.1	2.2	83.5	3.9
P12(74)-17	0.12558	0.00761	0.24521	0.01261	0.01416	0.00030	0.00745	0.00022	2037	103.4	222.7	10.3	90.6	1.9	149.9	4.4
P12(74)-18	0.04987	0.00433	0.08716	0.00704	0.01267	0.00026	0.00431	0.00014	189.1	190.1	84.9	6.6	81.2	1.6	86.9	2.7
P12(74)-19	0.07315	0.00332	0.43244	0.01521	0.04287	0.00067	0.01478	0.00030	1018	89.3	364.9	10.8	270.6	4.1	296.6	6.0
P12(74)-20	0.04998	0.00484	0.08715	0.00796	0.01264	0.00027	0.00402	0.00014	193.9	210.8	84.8	7.4	81.0	1.7	81.2	2.8
P12(74)-21	0.04983	0.00533	0.08617	0.00879	0.01254	0.00028	0.00390	0.00017	187	231.7	83.9	8.2	80.3	1.8	78.7	3.4
P12(74)-22	0.05002	0.00567	0.08618	0.0093	0.01249	0.00031	0.00411	0.00017	196	243.7	83.9	8.7	80.0	2.0	82.8	3.5
P12(74)-23	0.04805	0.00461	0.08545	0.00773	0.01290	0.00027	0.00414	0.00015	101.9	212.3	83.3	7.2	82.6	1.7	83.5	3.1
P12(74)-24	0.04616	0.00568	0.08228	0.00975	0.01293	0.0003	0.00451	0.00018	5.9	272.2	80.3	9.1	82.8	1.9	90.9	3.6

注：测试分析单位为西北大学大陆动力学国家重点实验室。

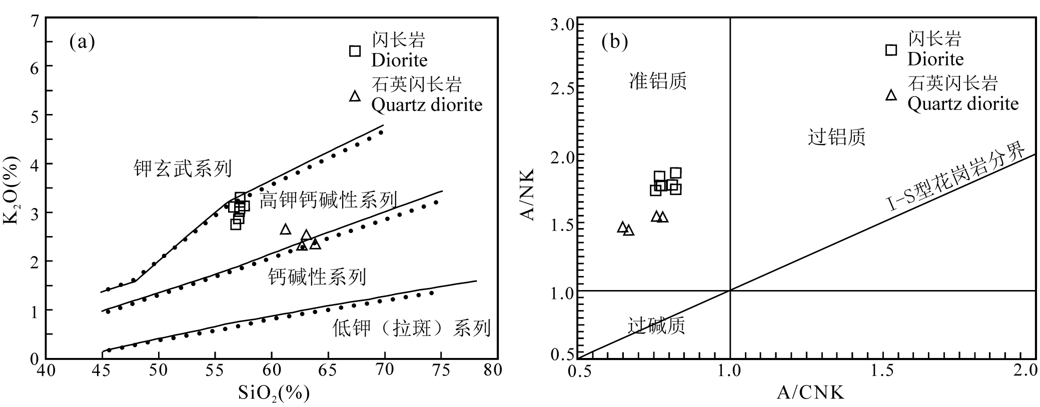

图 3 别若则错地区晚白垩世闪长岩 SiO_2-K_2O 图解(a，据汪晓伟等，2015；Peccerillo et al.，1976)和 A/CNK-A/NK 图解(b，据 Middlemost et al.，1986)

Fig. 3 SiO_2-K_2O diagram (a, after Wang Xiaowei et al., 2015; Peccerillo et al., 1976) and A/CNK-A/NK diagram (b, after Middlemost et al., 1986) for the Late Cretaceous diorite from Bieruozecuo area

4.2 稀土元素及微量元素

稀土元素及微量元素分析结果见表 1。闪长岩稀土元素总量为 $113.80\times10^{-6}\sim197.28\times10^{-6}$，$(La/Yb)_N$ 为 11.98～20.26，$\delta Eu=0.83\sim0.98$，岩石稀土含量值均略低于上地壳平均值(210.10×10^{-6})(Maniar et al.，1989)，球粒陨石标准化稀土元素分布模式表现为右倾稀土分布模式(图 4a)，具有不明显或弱负铕异常，La-Yb 和 Nd-Yb 之间具有良好的线性关系，显示了同源岩浆演化的特点(Wu Pengfei et al.，2013)。在原始地幔标准化蛛网图上

表 2　别若则错地区晚白垩世闪长岩主量元素(%)、微量元素($\times 10^{-6}$)及稀土元素($\times 10^{-6}$)分析结果

Table 2　Major (%), trace ($\times 10^{-6}$) and REE ($\times 10^{-6}$) elements analyses of the Late Cretaceous diorite from Bieruozecuo area

样号	P04(2)	P04(17)	P12(74)	P04(29)	P04(35)	P04(51)	P04(58)	P09(3)	P09(7)	P09(11)	P09(72)
岩性	闪长岩					石英闪长岩					
SiO_2	55.59	55.40	55.02	55.38	56.17	55.20	55.69	62.77	59.40	61.60	61.51
Al_2O_3	16.54	16.80	16.28	16.60	17.04	16.59	16.47	16.29	16.00	15.84	16.26
Fe_2O_3	2.72	2.50	2.54	3.57	2.73	2.86	2.76	2.46	2.69	2.68	2.41
FeO	4.47	4.32	4.78	3.75	4.08	4.34	4.41	1.92	2.65	2.14	2.36
CaO	5.30	5.74	6.08	5.15	5.32	6.25	6.26	4.00	4.97	4.64	4.89
MgO	3.80	3.38	3.86	3.80	3.41	3.68	3.64	2.39	3.15	2.48	2.59
K_2O	3.21	2.97	3.02	2.98	3.07	2.66	2.77	2.32	2.58	2.50	2.28
Na_2O	3.57	3.90	3.62	3.76	3.98	3.68	3.65	5.28	4.52	4.92	4.89
TiO_2	1.280	1.240	1.220	1.250	1.220	1.240	1.250	0.591	0.764	0.662	0.664
P_2O_5	0.400	0.414	0.372	0.402	0.387	0.398	0.391	0.227	0.297	0.245	0.255
MnO	0.118	0.111	0.13	0.123	0.11	0.116	0.117	0.078	0.114	0.114	0.088
LOI	2.28	2.40	2.34	2.62	1.81	2.22	1.89	1.07	2.19	1.54	1.17
H_2O^+	1.84	2.35	2.21	2.36	2.1	2.18	2.03	1.22	1.78	1.56	1.19
H_2O^-	0.136	0.126	0.192	0.161	0.147	0.112	0.076	0.244	0.228	0.134	0.197
CO_2	0.484	0.504	0.141	0.683	0.253	0.546	0.433	0.104	0.617	0.097	0.069
Total	99.458	99.755	99.465	99.969	100.017	99.852	99.947	99.894	99.76	99.612	99.653
σ	3.58	3.45	3.6	3.25	3.11	2.87	2.97	3.46	2.88	4.5	2.72
A/CNK	0.84	0.88	0.87	0.83	0.82	0.88	0.83	0.73	0.82	0.71	0.84
Cu	99.7	103	92.6	93.9	98.8	101	95.6	81.3	71.4	218	66.2
Pb	17.0	15.0	10.2	14.6	19.1	14.2	15.8	18.4	14.6	22.2	12.1
Zn	100.0	94.5	94.2	90.9	100.0	93.4	93.7	88.4	97.4	132	67.9
Cr	54.7	47.2	54.7	42.7	59.5	53.5	50.8	50.1	85.5	63.6	64.8
Ni	31.1	26.6	30.8	25.6	32.6	29.8	28.2	27.8	34.4	27.6	30.9
Co	22.9	22.4	20.8	20.3	24	22.9	22.7	13.6	17.8	15.8	16.2
Rb	119.0	102.0	76.4	105.0	86.6	86.4	85.8	67.1	72.7	73.0	70.5
Cs	2.15	3.52	1.22	1.88	1.55	2.28	1.90	0.82	1.05	0.78	1.84
W	14.7	13.0	8.54	12.2	13.6	11.2	12.8	17.4	17.4	13.8	27.5
Sb	1.14	0.94	0.6	2.49	0.63	0.76	1.78	1.23	1.51	2.21	0.71
Bi	0.026	0.028	0.052	0.091	0.05	0.028	0.045	0.2	0.052	0.14	0.059
Sr	521	582	520	543	530	622	574	568	654	628	711
Ba	577	496	358	504	436	452	416	597	589	540	540
V	175	167	184	172	204	193	200	92	124	99.4	105
Nb	19.1	18.7	16.1	17.9	17.9	17.9	18.1	8.97	11.9	11.9	11.5
Ta	1.12	1.1	1.16	1.06	1.05	1.05	1.07	0.56	0.71	0.76	0.72
Zr	253	243	192	233	231	238	233	98.9	85.1	132	84.3
Hf	5.81	5.59	5.34	5.5	5.47	5.44	5.44	2.63	2.42	3.38	2.55
Sn	1.83	2.06	2.04	1.87	1.68	1.76	1.92	1.18	1.36	1.00	1.35
Au	1.51	0.70	1.10	0.76	0.51	0.90	0.63	1.39	3.15	3.96	2.27
Ag	0.075	0.076	0.096	0.073	0.073	0.068	0.074	0.210	0.140	0.160	0.091
U	2.66	2.50	2.13	2.65	2.56	2.61	2.51	1.13	1.74	2.51	1.54
Th	12.2	11.6	8.36	11.5	11.2	11.4	11.3	7.16	9.48	11.2	9.66
Ti	0.741	0.715	0.728	0.724	0.706	0.721	0.724	0.342	0.442	0.383	0.384
La	42.9	42.5	41.9	41.1	38.0	41.4	41.3	28.6	33.8	33.3	31.8
Ce	75.6	75.0	76.4	75.5	66.6	72.6	71.5	44.2	54.0	52.0	51.4
Pr	10.40	10.40	9.78	10.00	9.38	10.00	9.85	5.80	7.22	6.70	6.65
Nd	41.5	40.7	38.1	41.1	37.4	40.1	40.1	21.9	28.1	26.2	25.7
Sm	7.69	7.50	7.10	7.41	6.98	7.36	7.30	3.86	5.01	4.32	4.33
Eu	1.93	1.90	1.84	1.91	1.82	1.90	1.89	1.17	1.41	1.27	1.29
Gd	6.30	6.40	5.89	6.35	5.84	6.20	6.19	3.36	3.89	3.72	3.81
Tb	0.87	0.86	0.83	0.79	0.80	0.84	0.85	0.41	0.50	0.48	0.48
Dy	4.45	4.54	4.49	4.43	4.27	4.46	4.45	2.02	2.63	2.31	2.39
Ho	0.82	0.86	0.88	0.78	0.80	0.82	0.78	0.36	0.48	0.42	0.42
Er	2.18	2.20	2.30	2.12	2.12	2.18	2.08	0.93	1.20	1.08	1.15
Tm	0.32	0.31	0.32	0.30	0.32	0.32	0.30	0.14	0.18	0.16	0.16
Yb	2.05	2.14	2.12	1.97	2.09	2.10	1.99	0.93	1.16	1.09	1.11
Lu	0.27	0.28	0.30	0.26	0.27	0.27	0.26	0.12	0.14	0.14	0.15
Y	19.8	20.5	20.5	19.0	19.7	19.9	19.3	9.03	11.3	10.0	10.5
$\sum$REE	197.28	195.59	192.25	194.02	176.69	190.55	188.84	113.80	139.72	133.19	130.84
δEu	0.83	0.83	0.85	0.84	0.86	0.85	0.85	0.98	0.95	0.95	0.96
$(La/Yb)_N$	13.79	13.08	13.02	13.74	11.98	12.99	13.67	20.26	19.19	20.13	18.87

注：测试单位为国土资源部武汉矿产资源监督检测中心武汉综合岩矿测试中心。

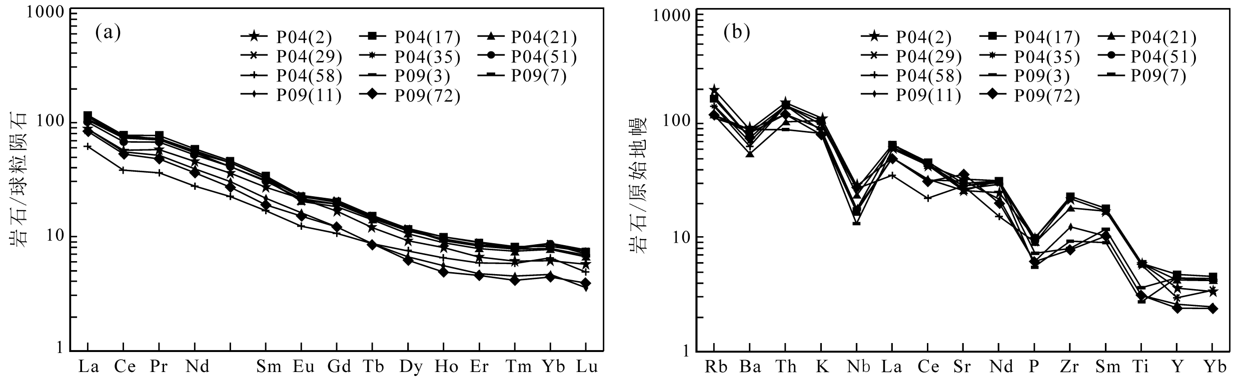

图 4 别若则错地区晚白垩世闪长岩稀土元素球粒陨石标准化配分曲线(a)和微量元素原始地幔标准化蛛网图(b)
(球粒陨石和原始地幔标准化值据 Masuda et al.,1973; Sun et al.,1989)

Fig. 4 Chondrite normalized REE pattern (a) and spider diagram of primitive mantle normalized trace elements (b) of the Late Cretaceous diorite from Bieruozecuo area (the standardized values of chondrites and primitive mantle after Masuda et al., 1973; Sun et al., 1989)

(图 4b),岩石大离子亲石元素(Rb、K)相对富集,大离子亲石元素(Ba)及高场强元素(Nb、P、Ce)相对亏损,具有弧型火山岩的地球化学特征(Mo Xuanxue et al.,2003),Nb 亏损反映岩浆受到了地壳物质的强烈混染或者可能与源区流体的交代作用有关(Jiang Yaohui et al.,2000; Kelemen et al.,2003; Zhong Huaming et al.,2006; Wu Pengfei et al.,2013)。Ba/Nb 值(22.2~66.6)变化大,而 Ba/Rb 值(4.7~8.9)稳定,说明岩石受后期的蚀变作用较弱(Zhang Ming et al.,1997),其主量和微量元素分析结果基本上代表了原始岩浆特征(Wu Pengfei et al.,2013)。

5 讨论

5.1 岩石成因

关于中性岩成因现今普遍认为有三种:幔源基性岩浆与花岗质岩浆的混合、幔源岩浆在 AFC(同化混染-分离结晶)过程中形成及地壳物质部分熔融形成(Arnaud et al.,1992; Thompson et al.,1996; Wang Yuejun et al.,2003)。钙碱性岩岩浆为壳幔混合源,花岗岩类型可划分富钾及钾长石斑状钙碱性花岗岩类(KCG)和含角闪石钙碱性花岗岩类(ACG)两类(Barbarin et al.,1999),KCG 高 K_2O、低 CaO,主要来源于地壳;ACG 低 K_2O、高 CaO,主要来源于地幔。别若则错地区晚白垩世闪长岩为准铝质高钾钙碱性岩,具高 K_2O(平均含量 2.76%)、低 CaO(平均含量 5.33%)特征,属 KCG 岩类,指示岩浆源地壳成分是主要的(肖庆辉等, 2002)。Nb、Ta 在侵蚀和变质作用过程中比较稳定,有示踪原始岩浆源区的特征(Barth et al., 2000; Pfander et al., 2007),区内晚白垩世闪长岩 Nb/Ta=13.88~17.05(平均 16.39),在幔源岩浆值(17±1)(Green, 1995)范围内;Nd/Th (1.75~5.60,平均 3.45)与壳源岩石值(≈3)相近,明显低于幔源值(>15)(Bea et al.,2001);Rb/Sr 值(0.099~0.228)低于地壳值(0.35),但远高于上地幔值(0.034)(Taylor et al.,1995),显示了壳幔混源的特点,Ti/Zr (29.0~45.6,平均 34.6)、Ti/Y (171.9~561.2,平均 358.4)略高于陆壳岩石(Ti/Zr<30,Ti/Y<200)(Wedepohl, 1995),可能与源区有石榴子石残留有关(Zhang Zunzhong et al.,2011)。岩石中微量元素 Cr ($42.7\times10^{-6}\sim85.5\times10^{-6}$,平均 57.0×10^{-6})、Ni ($25.6\times10^{-6}\sim34.4\times10^{-6}$,平均 29.6×10^{-6})、Co ($13.6\times10^{-6}\sim24.0\times10^{-6}$,平均 19.9×10^{-6})高于华北地台上陆壳值 Cr (52×10^{-6})、Ni (24×10^{-6})、Co (12×10^{-6})(鄢明才等,1997,2005;迟清华等,2007)。样品在 $(La/Yb)_N$-δEu 图(图 5a)中落入壳幔型范围。

由上述岩石地球化学分析可知,区内闪长岩成分具有明显的地幔和新生地壳双重特征,这种具有"集壳幔特性于一身"属性的岩浆岩在中冈底斯带内广泛发育(Ge et al.,2003)。同时,闪长岩具有不明显或弱负铕异常(δEu=0.83~0.98),结合 La/Sm-La 图解(图 5b)及岩体内可见暗色镁铁质包体,虽不能完全排除分离结晶的可能性,但部分熔融特征十分明显,其岩浆源可能是在俯冲和碰撞间地幔物质参与了地壳部分熔融形成的。

5.2 构造环境及地质意义

前人关于班公湖-怒江洋的俯冲及碰撞进程已

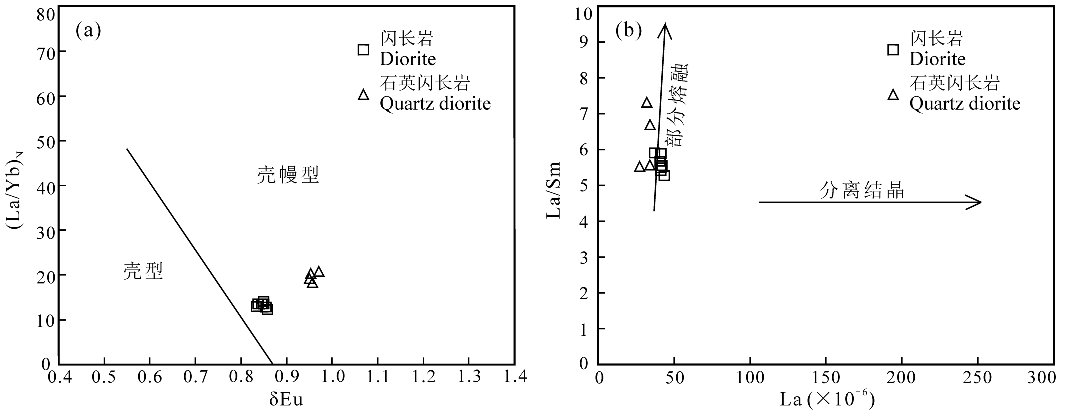

图 5　别若则错地区晚白垩世闪长岩(La/Yb)N-δEu 图(a，据邵拥军等，2003）和 La/Sm-La 图(b，据 Allegre et al.，1978)

Fig. 5　(La/Yb_N)-δEu diagram (a，after Shao Yongjun et al.，2003) and La/Sm-La diagram (b，after Allegre et al.，1978) of the Late Cretaceous diorite from Bieruozecuo area

有大量成果，亦有不同的争论。对班公湖-怒江中、西段晚中生代沉积、岩浆作用的详细研究（Fan Jianjun et al.，2018)，认为该区域班-怒洋关闭初始于晚侏罗世，早白垩世末期已完成向南俯冲，因此可认为班-怒特提斯洋的俯冲消减始于晚侏罗世以前，并持续至早白垩世晚期，最终在早白垩世晚期由东向西逐渐完成最终闭合，表明班-怒洋的活动具有明显的穿时性；结合在班公湖-怒江缝合带中—西段发现的早白垩世（115～120Ma）陆缘弧岩浆岩（Li Zhenyu et al.，2017；Ding Shuai et al.，2017）和晚白垩世早期（85～99Ma）碰撞造山岩浆岩（Li Guangming，2017；Zhang Zhi et al.，2017；Zheng Youye et al.，2017）的研究，进一步表明了班-怒洋的中—西段在早白垩世中早期尚未关闭。利用拉萨地体中部和北部早白垩世火山岩岩浆记录建立了该区同碰撞岩浆演化模式（Chen Shengsheng et al.，2017)，并认为早白垩世岩浆活动起因于拉萨地体与羌塘地块碰撞导致的岩石圈超常加厚，籍此表明雅江洋在早白垩世已完成洋陆转换，并发生地壳加厚；利用拉萨地块白垩纪岩浆记录，特别是富 K 钙碱性岩浆的活动时限研究，建立了班-怒洋俯冲-消减的地球动力学模式（Li Yalin et al.，2013，2017；Wang Qing at al.，2018；He Haiyang at al.，2018)，并以板片断离模式解释了该时期富 K 岩浆活动的动力学机制，表明 80～100Ma 期间，特别是 95～100Ma 之间拉萨-羌塘发生碰撞造山，并导致岩石圈加厚与上地壳缩短，洋陆转换造成地壳加厚发生在 96～91Ma (Zhang Xiangfei et al.，2011；Zhang Shuo et al.，2014)；雅鲁藏布洋打开时间不晚于晚三叠世，自中侏罗世开始向北俯冲形成俯冲型花岗岩类(127～70Ma)，约 70～65Ma 雅鲁藏布洋开始闭合，印度-亚洲大陆开始碰撞（Mo Xuanxue et al.，2005)。别若则错地区晚白垩世闪长岩体位于北冈底斯与中冈底斯过渡部位，本次对闪长岩进行的 LA-ICP-MS 锆石 U-Pb 年代学研究表明，岩体形成时代为 81.4±0.9Ma，为晚白垩世，该时期班公湖-怒江洋陆转换已经完成，进入后碰撞期，此时雅鲁藏布洋向北俯冲尚在进行中。该时期闪长岩在 R1-R2 图解（图 6a）中落入板块碰撞后隆起期花岗岩区域，在 Rb/30-Hf-3Ta 图解（图 6b）中主要落入火山弧范围内，两个样品落入碰撞后区域，在 Rb-(Y＋Nb)图解（图 6c）中落入火山弧花岗岩区域，暗示岩石形成于后碰撞的伸展环境，而与雅鲁藏布洋向北俯冲无关。班公湖-怒江缝合带在 96～91Ma 发生洋陆转换造成地壳加厚，其后在地幔软流底辟作用下，由前期俯冲和碰撞间产生的地壳发生线性热隆及薄化减压，从而地幔热能和物质参与了地壳部分熔融和热隆伸展，在 81Ma 左右形了区内闪长岩，岩体在就位过程中分离结晶作用不明显，其形成环境与扎隆琼娃石英二长岩相似（Li Hualiang et al.，2014)，样品显示的弧型火山岩特征是受岩石源区的影响。

6　结论

（1）别若则错地区晚白垩世闪长岩为准铝质高钾钙碱性系列岩石（KCG)。稀土元素分布模式上表现为右倾稀土分布模式，富集 K、Rb，亏损 Ba、Nb、P、Ce，类似于弧型火山岩特征。闪长岩地球化学成分具有明显的地幔和新生地壳双重特征，初步认为该类岩石是在地幔软流底辟作用下，由前期俯冲和碰撞间产生的地壳发生线性热隆及薄化减压，

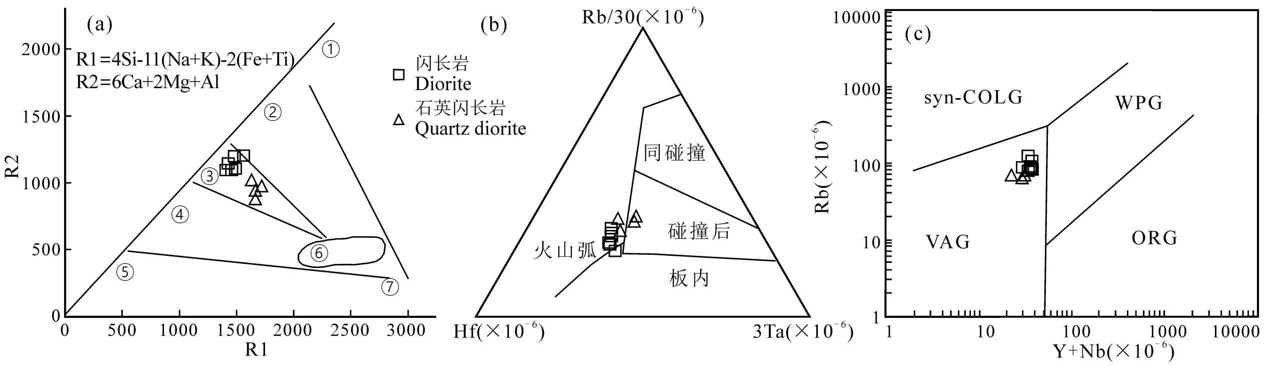

图 6 别若则错地区晚白垩世闪长岩 R1-R2 (a,据张硕等,2014),Rb/30-Hf-3Ta (b) 及 Rb-(Y+Nb)图解(c,据李华亮等,2014)

Fig. 6 R1-R2 (a, after Zhang Shuo et al., 2014), Rb/30-Hf-3Ta (b) and Rb-(Y+Nb) diagrams (c, after Li Hualiang et al., 2014) of the Late Cretaceous diorite from Bieruozecuo area

①—地幔斜长花岗岩;②—破坏性活动板块边缘(板块碰撞前)花岗岩;③—板块碰撞后隆起期花岗岩;④—晚造山期花岗岩;⑤—非造山区A型花岗岩;⑥—同碰撞(S型)花岗岩;⑦—造山期后A型花岗岩;VAG—火山弧花岗岩;Syn-COLG—同碰撞花岗岩;WPG—板内花岗岩;ORG—洋脊花岗岩

①—Mantle plagioclase granite; ②—destructive mobile plate margin (pre-collision) granite; ③—post collision uplift granite; ④—late orogenic granite; ⑤—anorogenic A-type granite; ⑥—syn-collision (S-type) granite; ⑦—post orogenic A-type granite; VAG—volcanic arc granite; Syn-COLG—syn-collision granite; WPG—within plate granite; ORG—ocean ridge granite

地幔热能和物质参与了地壳部分熔融和热隆伸展形成。

(2) 通过对闪长岩进行 LA-ICP-MS 锆石 U-Pb 测年,获得 81.4±0.9Ma (MSWD=0.55)岩石结晶年龄,形成时代为晚白垩世。

(3) 别若则错地区晚白垩世闪长岩形成于班公湖-怒江洋陆转换后的后碰撞的伸展环境。

致谢:本文参加工作的主要成员还有邵志伟、余旭辉、唐广成、朱国宝等,匿名审稿人提出宝贵修改意见,在此表示诚挚的感谢!

注 释

❶ 四川省地质矿产局区域地质调查队. 2016. 西藏改则别若则错 1:5 万 (I44E022020、I44E022021、I44E023020、I44E023021) 4 幅地质矿产调查报告.

References

Allegre C J, Minster J F. 1978. Quantitative method of trace element behavior in magmatic processes. Earth and Planetary Science Letters, 38: 1~25.

Arnaud N O, Vidal P, Tapponier P, et a1. 1992. The high K_2O volcanism of northwestern Tibet: Geochemistry and tectonic implications. Earth and Planetary Science Letters, 111: 351~367.

Barbarin B. 1999. A review of the relationship between granitoid types, their origins and their geodynamic environments. Lithos, (6): 483~492.

Barth M G, McDonough W F, Rudnick R L. 2000. Tracking the budget of Nb and Ta in the continental crust. Chemical Geology, 165(3): 197~213.

Bea F, Arzamastsev A, Montero P, Arzamastseva L. 2001. Aonmalous alkaline rocks of Soustov, Kola: Evidence of mantle-derived matasomatic fluids affecting crustal materials. Contributions to Mineralogy and Petrology, 140: 554~566.

Chen Shengsheng, Shi Rendeng, Gong Xiaohan, et al. 2017. A syn-collisional model for Early Cretaceous magmatism in the northern and central Lhasa subterranes. Gondwana Research, 41: 93~109.

Coulon C, Maluski H, Bollinger C, et al. 1986. Meszoic and Cenozoic volcanic rocks from central and southern Tibet: $^{39}Ar/^{40}Ar$ dating, petrological characteristics and geodynamical significance. Earth and Planetary Science Letters, 79: 281~302.

Ding Shuai, Tang Juxing, Zheng Wenbao, Yang Chao, Zhang Zhi, Wang Qin, Wang Yiyun. 2017. Geochronology and geochemistry of Naruo porphyry Cu (Au) deposit in Duolong ore-concentrated area, Tibet, and their geological significance. Earth Science, 42 (1): 1 ~ 23 (in Chinese with English abstract).

Fan Jianjun, Li Cai, Wang Ming, Xie Chaoming. 2018. Reconstructing in space and time the closure of the middle and western segments of the Bangong-Nujiang Tethyan Ocean in the Tibetan Plateau. International Journal of Earth Sciences, 107: 231~249.

Ge Liangsheng, Zou Yilin, Li Zhenghua, Zhang Xuejun, Huang Hui, Li Xingmou, Ma Jianwen. 2003. Geochemistry and genetic discussion of the granite in Bengnazangbu and Jiagang area, Tibet. Mineral. Petrol., 23(2): 55~61 (in Chinese with

English abstract).

Green T H. 1995. Significance of Nb/Ta as an indicator of geochemical processes in the crust-mantle system. Chemical Geology, 120(3): 347～359.

Harris N B W, Inger S, Xu R. 1990. Cretaceous plutonism in Central Tibet: An example of post-collision magmatism. Journal of Volcanology and Geothermal Research, 44: 21～32.

He Haiyang, Li Yalin, Wang Chengshan, et al. 2018. Late Cretaceous (ca. 95 Ma) magnesian andesites in the Biluoco area, southern Qiangtang subterrane, central Tibet: Petrogenetic and tectonic implications. Lithos, 302～303: 389～404.

Hou Kejun, Li Yanhe, Tian Yourong. 2009. In situ U-Pb zircon dating using laser ablation-multi ion counting-ICP-MS. Mineral Deposites, 28 (4): 481 ～ 492 (in Chinese with English abstract).

Jiang Yaohui, Yang Wanzhi. 2000. Geochemistry of early Yanshanian granitoids and its tectonic significance in the western Qinhai-Tibet plateau. Mineral. Petrol., 20(1): 74～79 (in Chinese with English abstract).

Kang Zhiqiang, Xu Jifeng, Dong Yanhui, Wang Baodi. 2008. Cretaceous volcanic rocks of Zenong Group in north-middle Lhasa block: Products of southward subducting of the Slainajap ocean? Acta Petrologica Sinica, 24(2): 303～314 (in Chinese with English abstract).

Kang Zhiqiang, Xu Jifeng, Wang Baodi, Dong Yanhui, Wang Shuqing, Chen Jianlin. 2009. Geochemistry of the Cretaceous Doni Group volcanic rocks in the northern of Lhasa: A tectonic setting. Earth Science, 34(1): 89～104 (in Chinese with English abstract).

Kapp P, DeCelles P G, Gehrel G E, et al. 2007. Geological records of the Lhasa-Qiangtang and Indo-Asian collisions in the Nima area of central Tibet. Geological Society of America Bulletin, 119(7-8): 917～933.

Kelemen P B, Hangh K, Greenem A R. 2003. One view of the geochemistry of subduction-related magmatic arcs, with an emphasis on primitive andesite and lower crust. In: Rudnick R L, ed. Treatise on Geochemistry. 3: 593～659.

Li Fenqi, Liu Wei, Zhang Shizhen, Li Yong. 2014. The evidence of earth dynamic background conversion in the north-central Gangdese and its adjacent regions during Middle Jurassic—Early Cretaceous. Geological Review, 60(6): 1297～1308 (in Chinese with English abstract).

Li Guangming, Qin Kezhang, Li Jinxiang, et al. 2017. Cretaceous magmatism and metallogeny in the Bangong-Nujiang metallogenic belt, central Tibet: Evidence from petrogeochemistry, zircon U-Pb ages, and Hf-O isotopic compositions. Gondwana Research, 41: 110～127.

Li Hualiang, Yang Shao, Li Dewei, Zhang Shuo, Lü Zhiwei, Chen Guifan. 2014. Geochronology, geochemistry, tectonic setting and metallogenetic significance of the Late Cretaceous quartz monzonite in the northwestern Gangdise terrane. Geotectonica et Metallogenia, 38(3): 694～705 (in Chinese with English abstract).

Li Yalin, He Juan, Wang Chengshan, et al. 2013. Late Cretaceous K-rich magmatism in central Tibet: Evidence for early elevation of the Tibetan plateau? Lithos, 160～161: 1～13.

Li Yalin, He Haiyang, Wang Chengshan, et al. 2017. Early Cretaceous (ca. 100 Ma) magmatism in the southern Qiangtang subterrane, central Tibet: Product of slab breakoff? International Journal of Earth Sciences, 106: 1289～1310.

Li Zhenyu, Ding Lin, Song Peiping, et al. 2017. Paleomagnetic constraints on the paleolatitude of the Lhasa block during the Early Cretaceous: Implications for the onset of India-Asia collision and latitudinal shortening estimates across Tibet and stable Asia. Gondwana Research, 41: 352～372.

Liu Wei, Li Fenqi, Yuan Sihua, Zhuo Jiewen, Zhang Wanping, Liang Ting. 2010. Zircon LA-ICP-MS U-Pb age of ignimbrite from Zenong Group in Coqen area of the central Gangdese belt, Tibet, China. Geological Bulletin of China, 29(7): 1009～1016 (in Chinese with English abstract).

Liu Yufei, Xu Jifeng, Zhang Zhaofeng, Wang Guiqin, Chen Jianlin, Huang Feng, Zhu Hongli, Liu Fang. 2018. Ca-Mg isotopic compositions of ultra-potassic volcanic rocks in the Lhasa terrane, southern Tibet and their geological implications. Acta Geologica Sinica, 92(3): 545～559 (in Chinese with English abstract).

Maniar P D, Piccli P M. 1989. Tectonic discrimination of granitoids. Geological Society of America Bulletin, 101(5): 635～643.

Masuda A, Nakamura N, Tanaka T. 1973. Fine structures of mutually normalized rare-earth patterns of chondrites. Geochimica et Cosmochimica Acta, 37(2): 239～248.

Meng Fancong, Xue Huaimin, Li Tianfu, Yang Huairen, Liu Fulai. 2005. Enriched characteristics of Late Mesozoic mantle under the Sulu orogenic belt: geochemical evidence from gabbro in Rushan. Acta Petrologica Sinica, 21: 1583～1592 (in Chinese with English abstract).

Middlemost E A K. 1986. Magmas and Magmatic Rocks: An Introduction to Igneous Petrology. London: Longman, 1～26.

Mo Xuanxue, Zhao Zhidan, Deng Jinfu, Dong Guochen, Zhou Su, Guo Tieying, Zhang Shuangquan, Wang Liangliang. 2003. Response of volcanism to the India-Asia collision. Earth Science Frontiers, 10(3): 135～148 (in Chinese with English abstract).

Mo Xuanxue, Dong Guochen, Zhao Zhidan, Zhou Su, Wang Liangliang, Qiu Ruizhao, Zhang Fengqin. 2005. Spatial and temporal distribution and characteristics of granitoids in the Gangdese, Tibet and implication for crustal growth and evolution. Geological Journal of China Universities, 11(3): 281～290 (in Chinese with English abstract).

Pan Guitang, Mo Xuanxue, Hou Zengqian, Zhu Dicheng, Wang Liquan, Li Guangming, Zhao Zhidan, Geng Quanru, Liao Zhongli. 2006. Spatial-temporal framework of the Gangdese orogenic belt and its evolution. Acta Petrologica Sinica, 22(3): 521～523 (in Chinese with English abstract).

Pearce J A, Mei H J. 1988. Volcanic rocks of the 1985 Tibet Geotraverse: Lhasa to Golmud. philosophical transactions of the Royal Society of London, Series A, Mathematical and Physical Sciences, 327(1594): 169～201.

Peccerillo R, Taylor S R. 1976. Geochemistry of Eocene calc-alkaline volcanic rocks from the Kastamonu area, northern Turkey. Contributions to Mineralogy and Petrology, 58(1): 63～81.

Pfander J A, Muinker C, Stracke A, et a1. 2007. Nb/Ta and Zr/Hf in ocean island basalts—implications for crust-mantle differentiation and the fate of Niobium. Earth and Planetary Science Letters, 254(1): 158～172.

Shao Yongjun, Peng Shenglin, Wu Ganguo, Zhang Da. 2003. The analysis on the rock-forming mechanism of Fenghuangshan rockbody in Tongling area. Geology and Exploration, 39(5): 35～43 (in Chinese with English abstract).

Shui Xinfang, He Zhanyu, Zhang Zeming, Lu Tianyu. 2016. Magmaorigin of Early Jurassic tonalites in the eastern Gandese magmatic belt, southern Tibet and its implications for the crustal evolution of the Lhasa terrane. Acta Geologica Sinica, 90(11): 3129～3152 (in Chinese with English abstract).

Sun S S, McDonough W F. 1989. Chemical and isotopic systematics of oceanic basalts: Implications for mantle composition and processes. In: Saunders A D, Norry M J, eds. Magmatism in the Ocean Basins. Geological Society, Special Publication, 42: 313～345.

Taylor S R, McLennan S M. 1995. The geochemical evolution of the continental crust. Reviews of Geophysics, 33(2): 241～265.

Thompson A B. 1996. Fertility of crusta1 rocks during anataxis. Transactions of Royal Society of Edinburgh. Earth Science, 87: 1～10.

Turner S P. 1996. Petrogenesis of the late-Delamerian gabboric complex at Black Hill, South Australia: Implications for convective thinning of the lithospheric mantle. Mineralogy and Petrology, 56: 51～89.

Wang Qing, Zhu Dicheng, Liu Anlin, et al. 2018. Survival of the Lhasa terrane during its collision with Asia due to crust-mantle coupling revealed by ca. 114 Ma intrusive rocks in western Tibet. Lithos, 304～307: 200～210.

Wang Xiaowei, Cui Fanglei, Sun Jiming, Zhu Xiaohui, Zhu Tao, Bai Jianke. 2015. Geochemical characteristics, geochronology and its geological significance of the diorite in Shagoukuduke area, East of the Bogda orogenic belt. Xinjiang Geology, 33(2): 151～158 (in Chinese with English abstract).

Wang Yuejun, Fan Weiming, Guo Feng, Liang Xinquan, Li Huimin. 2003. Geochemistry of early Mesozoic potassium-rich diorites-granodiorites in southeastern Hunan Province, South China: petrogenesis and tectonic implications. Geochemical Journal, 37(4): 427～448.

Wedepohl K H. 1995. The composition of the continental crust. Geochim. Cosmochim. Acta, 59: 1217～1232.

Wu Pengfei, Sun Deyou, Wang Tianhao, Gou Jun, Li Rong, Liu Wei, Liu Xiaoming. 2013. Chronology, geochemical characteristic and petrogenesis analysis of diorite in Helong of Yanbian area, NE China. Geological Journal of China Universities, 19(4): 600～610 (in Chinese with English abstract).

Yi Mingxiao, Zhao Yuanyi, Wang Ao, Xu Hong, Li Xiaosai, Lu Wei, Wang Xianwei. 2017. LA-MC-ICP-MS U-Pb dating of orthophyre from the Jiangcuo iron deposit in Baingoin County, Tibet and its geological significance. Acta Geologica Sinica, 91(5): 1039～1051 (in Chinese with English abstract).

Zeng Zhongcheng, Liu Demin, Wang Mingzhi, Zeren Zaxi, Nima Ciren, Zhang Ruoyu, Chen Ning, Zhu Weipeng. 2016. Tectoic-magmatic evolution and mineralization of the Qulong-Jiama areas in eastern section of Gangdese Mountains, Xizang (Tibet). Geological Review, 62(3): 663～678 (in Chinese with English abstract).

Zhang Ming, O'Reilly S Y. 1997. Multiple sources for basaltic rocks from Dubbo, eastern Australia: Geochemical evidence for plumelithospheric mantle interaction. Chemical Geology, 136(1-2): 33～54.

Zhang Shuo, Shi Hongfeng, Hao Haijian, Li Dewei, Lin Yan, Feng Minxuan. 2014. Geochronology, geochemistry and tectonic significance of Late Cretaceous adakites in Bangong Lake, Tibet. Journal of China University of Geosciences (Earth Science Edition), 39(5): 509～524 (in Chinese with English abstract).

Zhang Xiangfei. 2011. Characteristics and origin of the acid intrusive rocks in the Bangong ophiolitic melange zone in Ritu. Master thesis of Chengdu University of Technology, 35～45 (in Chinese with English abstract).

Zhang Yujie, Liu Wei, Zhu Tongxing, An Xianyin, Liao Zhongli. 2014. Zircon U-Pb age and geochemistry of Early Cretaceous intrusive rocks in Maiba area of Xainza County, Tibet. Geology in China, 41(1): 50～60 (in Chinese with English abstract).

Zhang Zhi, Song Junlong, Tang Juxing, Wang Liqaing, Yao Xiaofeng, Li Zhijun. 2017. Petrogenesis, diagenesis and mineralization ages of Galale Cu-Au deposit, Tibet: Zircon U-Pb age, Hf isotopic composition and molybdenite Re-Os dating. Earth Science, 42(6): 862～880 (in Chinese with English abstract).

Zhang Zunzhong, Gu Lianxing, Wu Changzhi, Di Jianping, Wang Chuansheng, Tang Junhua, Xiao E. 2011. Early-Middle Indosinian Weiya quartz diorite, eastern segment of the Middle Tianshan Mountains, NW China: Implications for intra-continent subduction and partial melting of juvenile lower crust. Acta Geologica Sinica, 85(9): 1420～1434 (in Chinese with English abstract).

Zheng Youye, Ci Qiong, Wu Song, Jin Liangxu, Guo Jianci, Ci Renji, Gong Fuzhi, Tan Meng, Zhang Hongqiang. 2017. The discovery and signigicance of Rongga porphyry Mo deposit in the Bangong-Nujiang metallogenic belt, Tibet. Earth Science, 42

(9): 1441～1453 (in Chinese with English abstract).

Zhong Huaming, Tong Jinsong, Lu Rukui, Xia Jun. 2006. Geochemical characteristics and tectonic setting of peraluminous granite in the Songxi area, Rutog County, Tibet, China. Geological Bulletin of China, 25(2): 183～188 (in Chinese with English abstract).

Zhou Hua, Qiu Jiansheng, Yu Sibin, Wang Ruiqiang. 2016. Geochronology and geochemistry of volcanic rocks from Coqen district of Tibet and their implications for petrogenesis. Acta Geologica Sinica, 90(11): 3173～3191 (in Chinese with English abstract).

Zhu D C, Chung S L, Mo X X, et al. 2009. The 132 Ma Comei Bunbury large igneous province: Remnants identified in present day southeastern Tibet and southwestern Australia. Geology, 37 (7): 583～586.

Zhu D C, Zhao Z D, Niu Y L, et al. 2011. The Lhasa terrane: Record of a microcontinent and its histories of drift and growth. Earth and Planetary Science Letters, 301(1): 241～255.

Zhu Dicheng, Pan Guitang, Mo Xuanxue, Wang Liquan, Liao Zhongli, Zhao Zhidan, Dong Guochen, Zhou Changyong. 2006. Late Jurassic-Early Cretaceous geodynamic setting in middle-northern Gangese: New insights from vocalnic rocks. Acta Petrologica Sinica, 22(3): 534～546 (in Chinese with English abstract).

Zhu Dicheng, Pan Guitang, Wang Liquan, Mo Xuanxue, Zhao Zhidan, Zhou Changyong, Liao Zhongli, Dong Guochen, Yuan Sihua. 2008a. Spatial-temporal distribution and tectonic setting of Jurassic magmatism in the Gangdise belt, Tibet. China. Geological Bulletin of China, 27(4): 458～468 (in Chinese with English abstract).

Zhu Dicheng, Pan Guitang, Wang Liquan, Mo Xuanxue, Zhao Zhidan, Zhou Changyong Liao Zhongli, Dong Guochen, Yuan Sihua. 2008b. Tempo-spatial variations of Mesozoic magmatic rocks in the Gangdise belt, Tibet, with a discussion of geodynamic setting-related issues. Geological Bulletin of China, 27(9): 1535～1550 (in Chinese with English abstract).

Zhu Dicheng, Mo Xuanxue, Zhao Zhidan, Xu Jifeng, Zhou Changyong, Sun Chenguang, Wang Liquan, Chen Haihong, Dong Guochen, Zhou Su. 2008c. Zircon U-Pb geochronology of Zenong Group volcanic rocks in Coqen area of the Gangdese, Tibet and tectonic significance. Acta Petrologica Sinica, 24(2): 1～12 (in Chinese with English abstract).

参　考　文　献

迟清华，鄢明才. 2007. 应用地球化学元素丰度数据手册. 北京:地质出版社，101～102.

丁帅，唐菊兴，郑文宝，杨超，张志，王勤，王艺云. 2017. 西藏拿若斑岩型铜（金）矿含矿岩体年代学、地球化学及地质意义. 地球科学，42(1):1～23.

葛良胜，邹依林，李振华，张学军，黄辉，李兴谋，马建文. 2003. 西藏崩纳藏布和甲岗雪山地区花岗岩的地球化学特征及成因初探. 矿物岩石，23(2):55～61.

侯可军，李延河，田有荣. 2009. LA-MC-ICP-MS 锆石微区原位 U-Pb 定年技术. 矿床地质，28(4): 481～492.

姜耀辉，杨万志. 2000. 青藏高原西部燕山早期花岗岩地球化学及其大地构造意义. 矿物岩石，20(1):74～79.

康志强，许继峰，董彦辉，王保弟. 2008. 拉萨地块中北部白垩纪则弄群火山岩 Slainajap 洋向南俯冲的产物. 岩石学报，24(2): 303～314.

康志强，许继峰，王保弟，董彦辉，王树庆，陈建林. 2009. 拉萨地块北部白垩纪多尼组火山岩的地球化学:形成的构造环境. 地球科学，34(1): 89～104.

李奋其，刘伟，张士贞，李勇. 2014. 冈底斯中北部及邻区中侏罗世—早白垩世地球动力背景转换的证据. 地质论评，60(6): 1297～1308.

李华亮，杨绍，李德威，张硕，吕志伟，陈桂凡. 2014. 冈底斯西北缘晚白垩世石英二长岩的年代学、地球化学、构造环境及成矿意义. 大地构造与成矿学，38(3):694～705.

刘伟，李奋其，袁四化，卓皆文，张万平，梁婷. 2010. 西藏中冈底斯带措勤地区则弄群熔结凝灰岩锆石 LA-ICP-MS U-Pb 年龄. 地质通报，29(7):1009～1016.

刘峪菲，许继峰，张兆峰，王桂琴，陈建林，黄丰，祝红丽，刘芳. 2018. 青藏高原拉萨地块中西部超钾质岩 Ca-Mg 同位素特征及其地质意义. 地质学报，92(3):545～559.

孟繁聪，薛怀民，李天福，杨怀仁，刘福来. 2005. 苏鲁造山带晚中生代地幔的富集特征——来自辉长岩的地球化学证据. 岩石学报，21:1583～1592.

莫宣学，赵志丹，邓晋福，董国臣，周肃，郭铁鹰，张双全，王亮亮. 2003. 印度-亚洲大陆主碰撞过程的火山作用响应. 地学前缘，10(3):135～148.

莫宣学，董国臣，赵志丹，周肃，王亮亮，邱瑞照，张风琴. 2005. 西藏冈底斯带花岗岩的时空分布特征及地壳生长演化信息. 高校地质学报，11(3):281～290.

潘桂棠，莫宣学，侯增谦，朱弟成，王立全，李光明，赵志丹，耿全如，廖忠礼. 2006. 冈底斯造山带的时空结构造及演化. 岩石学报，22(3):521～523.

邵拥军，彭省临，吴淦国，张达. 2003. 铜陵凤凰山岩体成岩机制探讨. 地质与勘探，39(5):35～43.

水新芳，贺振宇，张泽明，陆天宇. 2016. 西藏冈底斯带东段早侏罗世英云闪长岩的岩浆起源及其对拉萨地体地壳演化的意义. 地质学报，90(11):3129～3152.

肖庆辉，邓晋福，马大铨，等. 2002. 花岗岩研究思维与方法. 北京:地质出版社，12～20.

汪晓伟，崔方磊，孙吉明，朱小辉，朱涛，白建科. 2015. 博格达造山带东段沙沟库都克闪长岩体地球化学特征、年代学及地质意义. 新疆地质，33(2):151～158.

武鹏飞，孙德有，王天豪，苟军，李蓉，刘玮，柳小明. 2013. 延边和龙地区闪长岩的年代学、地球化学特征及岩石成因研究. 高校地质学报，19(4):600～610.

鄢明才，迟清华. 1997. 中国东部大陆地壳与岩石的化学组成. 北京:科学出版社，1～292.

鄢明才，迟清华. 2005. 中国东部大陆地壳与岩石的化学组成. 北京:科学出版社，1～174.

易明筱，赵元艺，汪傲，许虹，李小赛，卢伟，王贤伟. 2017. 西藏班戈县江错铁矿正长斑岩锆石 LA-MC-ICP-MS U-Pb 定年及意义. 地质学报，91(5)：1039～1051.

曾忠诚，刘德民，王明志，泽仁扎西，尼玛次仁，张若愚，陈宁，朱伟鹏. 2016. 西藏冈底斯东段驱龙—甲马地区构造-岩浆演化与成矿. 地质论评，62(3)：663～678.

张硕，史洪峰，郝海健，李德威，斉岩，冯旻譞. 2014. 青藏高原班公湖地区晚白垩世埃达克岩年代学、地球化学及构造意义. 地球科学——中国地质大学学报，39(5)：509～524.

张向飞. 2011. 班公湖蛇绿混杂岩带酸性侵入岩特征及成因. 成都：成都理工大学硕士学位论文，35～45.

张予杰，刘伟，朱同兴，安显银，廖忠礼. 2014. 西藏申扎县买巴地区早白垩世侵入岩锆石 U-Pb 年龄及地球化学. 中国地质，41(1)：50～60.

张志，宋俊龙，唐菊兴，王立强，姚晓峰，李志军. 2017. 西藏嘎拉勒铜金矿床的成岩成矿时代与岩石成因：锆石 U-Pb 年龄、Hf 同位素组成及辉钼矿 Re-Os 定年. 地球科学，42(6)：862～880.

张遵忠，顾连兴，吴昌志，翟建平，汪传胜，唐俊华，肖娥. 2011. 中天山东段尾亚印支早—中期石英闪长岩——陆内俯冲与原生下陆壳部分熔融. 地质学报，85(9)：1420～1434.

郑有业，次琼，吴松，晋良旭，郭建慈，次仁吉，龚福志，谭勐，张弘强. 2017. 西藏班公湖-怒江成矿带荣嘎斑岩型钼矿床的发现及意义. 地球科学，42(9)：1441～1453.

钟华明，童劲松，鲁如魁，夏军. 2006. 西藏日土县松西地区过铝质花岗岩的地球化学特征及构造背景. 地质通报，25(2)：183～188.

周华，邱检生，喻思斌，王睿强. 2016. 西藏措勤地区火山岩的年代学与地球化学及其对岩石成因的制约. 地质学报，90(11)：3173～3191.

朱弟成，潘桂棠，莫宣学，王立全，廖忠礼，赵志丹，董国臣，周长勇. 2006. 冈底斯中北部晚侏罗世—早白垩世地球动力学环境：火山岩约束. 岩石学报，22(3)：534～546.

朱弟成，潘桂棠，王立全，莫宣学，赵志丹，周长勇，廖忠礼，董国臣，袁四化. 2008a. 西藏冈底斯带侏罗纪岩浆作用的时空分布及构造环境. 地质通报，27(4)：458～468.

朱弟成，潘桂棠，王立全，莫宣学，赵志丹，周长勇，廖忠礼，董国臣，袁四化. 2008b. 西藏冈底斯带中生代岩浆岩的时空分布和相关问题的讨论. 地质通报，27(9)：1535～1550.

朱弟成，莫宣学，赵志丹，许继峰，周长勇，孙晨光，王立全，陈海红，董国臣，周肃. 2008c. 西藏冈底斯带措勤地区则弄群火山岩锆石 U-Pb 年代学格架及构造意义. 岩石学报，24(2)：1～12.

LA-ICP-MS Zircon U-Pb Dating and Geochemical Analysis of the Late Cretaceous Diorite in the Bieruozecuo Area, Northwestern Margin of the Gangdise Belt, Tibet, and Their Geological Significances

QIU Chanyuan[1)], XIAO Qianru[1)], WEI Yongfeng[1,2)], LUO Wei[1,2)], YANG Yamin[1)], XIAO Yuanfu[1)]

1) *College of Earth Sciences, Chengdu University of Technology, Chengdu*, 610059;

2) *Regional Geological Survey Team, Sichuan Geology and Mineral Bureau, Shuangliu, Sichuan*, 610213

Abstract

Diorite in the Bieruozecuo area of Tibetoccurs in the Early Cretaceous Qushenla Group or intermediate-felsic rocks as irregular or elliptic stocks, with minor mafic enclaves. LA-ICP-MS zircon U-Pb dating of the diorite yields a crystallization age of 81.4±0.9 Ma (MSWD=0.55), suggesting late Cretaceous age for magmatic activity. Geochemical analysis shows that the diorite is rich in K_2O and poor in CaO, and should belong to quasi aluminum, high K and Ca, alkaline series rock (KCG). The total amount of rare earth elements ranges from 113.80×10^{-6} to 197.28×10^{-6}, with $(La/Yb)_N$ of 11.98～20.26 and the δEu of 0.83 to 0.98. Chondrite normalized REE patterns show relative enrichment of LREE, right-dipping distribution trend, and no obvious Eu depletion. Primitive mantle normalization spider diagram reveals enrichment of K and Rb and depletion of Nb and P, and these features are similar to that of arc volcanic rocks. Geochemical compositions of the diorite show double features of mantle and newly-formed crust, indicating that the diorite likely resulted from linear thermal uplift and thinning decompression of the crust under the effect of mantle flow diaperism in the early stage of subduction and collision. The mantle thermal energy and materials, together with partial melting of the crust, resulted in the formation the diorite in the post collision-extension environment during the ocean-continent transition of the Bangonghu-Nujiang suture zone.

Key words: northwestern margin of Gangdise; Late Cretaceous; diorite; LA-CP-MS zircon U-Pb dating